ISSN 2347-6893
Volume 9 Number2
Journal of Advances in Biology

Reorganization of the cytoskeleton

Gyula Vincze[1], Gyula Peter Szigeti[2], Andras Szasz[1]
[1]Department of Biotechnics, St. Istvan University, Budapest, Hungary
biotech@gek.szie.hu
[2]Institute of Human Physiology and Clinical Experimental Research, Semmelweis University, Budapest, Hungary
szigeti.gyulapeter@gmail.com

ABSTRACT

The effect of a modulated electromagnetic field on the cytoskeleton is possible through the action of voltage-sensitive phosphatase (VSP). Field-controlled phosphorous hydrolysis could have important roles in cytoskeleton restructuring, as well as in resonant-type behavior.

Indexing terms/Keywords

cytoskeleton

INTRODUCTION

The voltage-sensitive phosphatase (VSP) [1] is sensitive to external fields and at the same time acts in the cytosol, where it allows the transfer of the external field effect into the cell interior. This generates biochemical signals that could play a role in intracellular organization. Through these signals, we should be able to generate biochemical signals in the cytosol to control some internal processes, most probably the polymerization of the cytoskeleton. The basic mechanism is that membrane depolarization hydrolyzes phosphoinositol [2]. This process is mediated by the transformation of $PtdIns(3,4,5)P_3$ to $PtdIns(3,4,5)P_2$ and releases one molecule of phosphorous into the cytosol.

Based on this mechanism [2], the chemical reaction is as follows:

$$PtdIns(3,4,5)P_3 \underset{\beta}{\overset{\alpha}{\rightleftarrows}} PtdIns(3,4,5)P_2 \qquad (1)$$

This is a reversible decomposition reaction, where the reaction rates α and β can be modified by the membrane potential, and through this mechanism by the external electric field. In this study, we will show induced stochastic resonance by the action of an external AC field. Furthermore, multiple processes are generated in the cytosol, including local $PtdIns(3,4,5)P_2$, which controls the cytoskeletal network. This control is based on the activation/deactivation of microtubule-associated proteins (MAPs) by phosphorous. The phosphorylation of MAP destabilizes microtubules by weakening their internal bonds [3].

One of the differences between quiescent and proliferative cells is the lower absolute value of the membrane potential of the latter [4]. This low membrane potential especially characterizes malignant cells [5]. This means that cancerous cells are permanently in a depolarized state, so their VSPs keep the level of $PtdIns(3,4,5)P_2$ molecules high, which influences their cytoskeleton. The low level of cytoskeletal polymerization ensures the higher mobility of malignant cells. The presence of $PtdIns(3,4,5)P_2$ is essential for the proper function of numerous ion channels and transporters as well as for moving vesicles. This mechanism mediates the active influence of an external electric field on cell intercellular electrolyte levels and protein connections. An increase the concentration of $PtdIns(3,4,5)P_2$ stimulates the operation of phosphorous-sensitive KCNQ potassium channels and inhibits the operation of the SNC5A8 sodium co-transporter. This dynamic stability is governed by the Le Chatelier principle: a sudden change (e.g. drop) in membrane potential generates phosphorylation and increases the transport of potassium in parallel with the suppression of sodium transport; this complex process tries to maintain the original membrane potential. This effectively interacts with the proliferation process. The SNC5A8 sodium co-transporter reduces the concentration of co-transported mono-carboxylate, which reduces the concentration of butyrate in the vicinity of histone deacetylase (HDAC), stimulating its activity, and

DOI : 10.24297/jab.v9i2.4059

consequently the rate of proliferation increases [6].SLC5A8 is also a tumor suppressor, and is inactive in proliferating tumors. Phosphorylation influences this suppressor.

A few processes where VSP could play a role

Role of VSP in anaerobic glycolysis and cancerous transformation

The effect of stress on homeostatic control generally activates the production of chaperone stress proteins. This production consumes ATP, and in this way decreases the ATP-dependent active membrane transport of ions, causing depolarization of the cell membrane. The phosphorylation of VSP is activated by this process. This effect decreases the activity of the SLC5A8 tumor suppressor, and so the rate of proliferation increases. However, this further increases the demand for ATP, which cannot be produced in sufficient amounts by mitochondria. Thus, a process with higher energy flux is mandatory. This is known to occur in sport medicine, when a lack of oxygen for muscle activity initiates high energy-flux anaerobic fermentative ATP production, which is regulated back to the normal level after activity ceases. However, in this case, when the stress is permanent and the cells are not able to escape from the demand of high energy-flux, oncogenes may be activated, which could be promoted by the inhibition of apoptosis and high concentrations of stress proteins. This situation is ideal for the development of cancer. The prolonged, unrecognized precancerous stage is likely characterized by this process battling with normal homeostatic regulation.

One of the most characteristic tumor suppressor genes is PTEN, which interacts enzymatically with processes in the cytosol. This interaction is partly homologue to cytosolic part of VSP [7]. Note that the substrate of PTEN is phosphorous in the cell membrane, so it must come into contact with the membrane to mediate its activity. This could be a further coupling between PTEN and VSP. It is likely that an external electric field influences this coupling.

Role of VSP in reorganization (polymerization) of the cytoskeleton

Cytoskeleton fibers follow the electric field [8], so direct current reorganizes the cytoskeleton [9]. Alternative current (AC) fields also reorganize the cytoskeleton, with the greatest influence at around 1 Hz [10]. This represents some kind of resonant effect with AC. We have shown that stochastic resonance [11] could describe this phenomenon, assuming a bistable two-position VSP state (similar to voltage-gated ion channels).

To understand the underlying physics of stochastic resonance, we considered a bifurcative (bistable) potential-well. The noise constrains the particle to randomly oscillate in this double-well, and the time spending in one of the wells is a probability variable of time (P(t)) with an exponential distribution function:

$$P(t) = \frac{1}{T_K} e^{-\frac{t}{T_K}} \tag{2}$$

The value of TK occupation time (so called Kramer's time-scale) is determined by the generalized Arrhenius factor weighted by the average frequency f:

$$T_K(D) = \frac{1}{f} e^{-\frac{\Delta U}{D}} \tag{3}$$

Where the ΔU is the depth of the potential well and D is the average energy of the noise (if it is thermal, then D=kT). If the particle in the double well is under a periodic force Acos(Ωt) (where the amplitude A is small compared to ΔU; A<< ΔU/D), then the coupled wells periodically fluctuate up and down in opposite phase.

At time t=0, the jump from right to left is more probable than at time t=π/2Ω, and opposite at time t=π/Ω. This means that the weak periodic signal (much weaker than the activation energy) synchronizes the jumps, but of course in a stochastic (and not deterministic) way. The stochastic resonance occurs at D*, when Kramer's time is one half of the period time of the weak deterministic signal:

$$D^* = \frac{\Delta U}{\ln\left(\frac{\pi f}{\Omega}\right)} \tag{4}$$

Consequently, the distribution function of the jumping time in the case of the noise modulated with a weak periodic signal will not be a rigorously monotonic decreasing function as in (3), but will have definite periods by maxima:

$$t_{\max} = (2n+1)\frac{\pi}{\Omega} \tag{5}$$

and a considerable amplification of the weak periodic signal can be observed depending on the D* noise. The amplification also increases with decreasing frequency (at constant amplitude A). It is interesting that the amplification increases with decreasing amplitude A at the same signal frequency, and suddenly (at a threshold), the resonance disappears (the window phenomenon). This is likely the reason for the Adey window [12].

By more rigorous calculations using Fokker-Plank equations:

the amplification of the system (η) is definitely determined at the frequencies fr=(Ω/2 π),

the spectral power density function has needle-like (similar to Dirac delta) peaks at frequencies (n fr) where n is an integer,

the power of these peaks depends on the amplitude A and noise power D.

The stochastic resonance can be easily shown using a simple dynamic system, i.e. an over-smoothed non-linear oscillator, which can be described by the motion equation:

$$\frac{dx}{dt} = -\frac{dU(x)}{dx} + F(t) + aA(x)\cos(\Omega t + \varphi_0) \tag{6}$$

where the U(x) potential has two stable and one unstable (the middle) minima at X-, X+ and X0; F(t) is a random force (assumed for simplicity as white noise with s normal distribution and power D, A(x)cos(Ωt+φ0) and the exciting deterministic (periodic) signal; a is constant.

The random force constrains the oscillation between the two stable states, so it jumps through the potential barrier:

$$\Delta U^{\pm} = U(X_0) - U(X^{\pm}) \tag{7}$$

The kinetics of the transition are determined by the height of the barrier (ΔU±), and the power D of the noise. The time τ± to stay at the actual minima (and the 1/τ±=r± transition rate) is determined from Kramer's equation (3):

$$\frac{1}{\tau^{\pm}} = r^{\pm} = \frac{1}{2\pi}\sqrt{-\left.\frac{\partial^2 U(x)}{\partial x^2}\right|_{x=X_0}\left.\frac{\partial^2 U(x)}{\partial x^2}\right|_{x=X^{\pm}}}\, e^{-\frac{\Delta U^{\pm}}{D}} \tag{8}$$

The periodic potential will be modulated by time and its value oscillates at point X± in the opposite phase due to the periodic force:

$$W(x,t) = U(x) - aG(x)\cos(\Omega t + \varphi_0) \qquad \left\{A(x) = \frac{dG(x)}{dx}\right\} \tag{9}$$

When D is small, the Fokker-Plank equation for the adiabatic approach for points X+ and X- is reduced to the probability master equation:

$$\frac{dp_+(t)}{dt} = r_-(t)p_-(t) - r_+(t)p_+(t) \qquad \{p_+(t) + p_-(t) = 1\} \tag{10}$$

The values of r± can be determined from equation (8), substituting W instead of U. When A(x)=1, the potential becomes simple:

$$U(x) = -\lambda\frac{x^2}{2} + \frac{x^4}{4} \qquad \left\{\lambda > 0, \qquad \left[X_0 = 0, \qquad X^{\pm} = \pm\lambda^{\frac{1}{2}}\right]\right\} \tag{11}$$

Hence from (10) we get:

$$\delta p(t) = A(D)\cos(\Omega t + \varphi + \psi) \tag{12}$$

where the A(D) amplitude and the ψ phase-shift are:

$$A(D) = a\frac{\lambda}{D}\frac{r(D)}{\sqrt{r^2(D) + \frac{\Omega^2}{4}}}, \qquad \psi = -artg\left(\frac{\Omega}{2r(D)}\right), \tag{13}$$

$$r(D) = r_+ = r_- = \frac{\lambda}{\sqrt{2\pi}}e^{-\frac{\lambda^2}{2D}}$$

The amplitude exhibits resonance-like behavior; in the case D=kT, we are speaking about thermal noise. The maximum depends on D noise amplitude or at D=const. The maximum is determined by the frequency. This is the typical frequency-amplitude window formulated based on experiments [12].

The reorganization patterns of the cytoskeleton are different for DC and AC

In case of a DC field, the two sides of the cells are oppositely polarized, i.e. one is hyperpolarized the opposite side depolarized. Depolarization hydrolyzes phosphorous, and thus initiates the formation of the cytoskeleton on the hyperpolarized side. This gradient connecting the two opposite polarizations forms a pattern similar to the electromagnetic field. In the case of AC excitation, both poles are in stochastic resonance (simply referred to as north and south), and both are hyperpolarized, inducing reorganization. On the other hand, the east and west poles have no resonance, so phosphorylation is normal, and the general gradient of phosphorous shows an east-west direction. The reorganization of the cytoskeleton has a definite driving force, building a pattern perpendicular to the DC-induced one.

Explanation of resonance-like cytoskeleton reorganization by an AC field

Denote the two chemical components with A and B in (1), for simplicity. In this case, the reversible decomposition reaction of (1) will be:

$$A \underset{\beta}{\overset{\alpha}{\rightleftarrows}} B \tag{14}$$

The concentrations of the components are denoted by $[A]$ and $[B]$. So, based on (14), the kinetic equation will be:

$$\frac{d[A]}{dt} = -\alpha[A] + \beta[B] \tag{15}$$

$$\frac{d[B]}{dt} = \alpha[A] - \beta[B]$$

ISSN 2347-6893
Volume 9 Number2
Journal of Advances in Biology

Where αand βare the forward and reverse reaction rates. Reorganizing equation (15) into a more convenient form, let us introduce the values of $[T]=[A]+[B], \quad p_1=[A]/[T], \quad p_2=[B]/[T]$.

Thus, (15) will be transformed into the master equation:

$$\frac{dp_1}{dt}=-\alpha p_1+\beta p_2 \tag{16}$$
$$\frac{dp_1}{dt}=\alpha p_1-\beta p_2,$$
$$p_1+p_2=1$$

To express the mathematical formula for $p_i,(i=1,2)$ concentrations, consider the stationary state of (16), when $\frac{dp_i}{dt}=0$. Hence:

$$\frac{p_1}{p_2}=\frac{\beta}{\alpha} \tag{17}$$

When $\pm\Delta E$ are the deviations from the reference level, we assume the Boltzmann distribution:

$$\frac{p_1}{p_2}=\frac{\beta}{\alpha}=\frac{e^{-\frac{E_0+\Delta E}{kT}}}{e^{-\frac{E_0-\Delta E}{kT}}} \tag{18}$$

From where the reaction rates follow the Arrhenius law:

$$\alpha=Ce^{-\frac{E_0-\Delta E}{kT}}, \quad \beta=Ce^{-\frac{E_0+\Delta E}{kT}} \tag{19}$$

Hence, for example calculating p_1 from (16), we obtain the following differential equation:

$$2\tau\frac{dp_1}{dt}=-(e^{\frac{\Delta E}{kT}}+e^{-\frac{\Delta E}{kT}})p_1+e^{-\frac{\Delta E}{kT}}, \tag{20}$$
$$2\tau=\left(Ce^{-\frac{E_0}{kT}}\right)^{-1}$$

By expanding in the exponentials and stopping at the first order, the following linear differential equation is the result:

$$\frac{dp_1}{dt} = -\frac{1}{\tau} p_1 + \frac{1}{2\tau} - \frac{1}{2\tau}\frac{\Delta E}{kT}, \qquad (21)$$

$$2\tau = \left(Ce^{-\frac{E_0}{kT}} \right)^{-1}$$

When the strength of the electric field is a harmonic function over time, and the energy depends on it linearly, we write:

$$\Delta E = a \sin \omega t \qquad (22)$$

And, consequently, the differential equation of the concentration is simplified:

$$\frac{dp_1}{dt} = -\frac{1}{\tau} p_1 + \frac{1}{2\tau} - \frac{1}{2\tau}\frac{a}{kT}\sin \omega t \qquad (23)$$

For further study this, when we are interested in the answer for harmonic excitation, we have to solve the stationary situation:

$$\frac{dp}{dt} + \frac{1}{\tau} p = -\frac{1}{2\tau}\frac{a}{kT}\sin \omega t \qquad (24)$$

The concentration following equation (24) has to change by a harmonic function over time and its amplitude depends on the kT noise strength:

$$\hat{p}(RT) = \frac{a}{2kT}\frac{1}{\sqrt{\tau^2\omega^2 + 1}} = \frac{a}{2kT}\frac{1}{\sqrt{1 + \left(\frac{e^{\frac{E_0}{RT}}}{2C}\omega \right)^2}} \qquad (25)$$

This function in (25) has a sharp maximum at a given frequency, depending on the noise strength (Figure 1.).

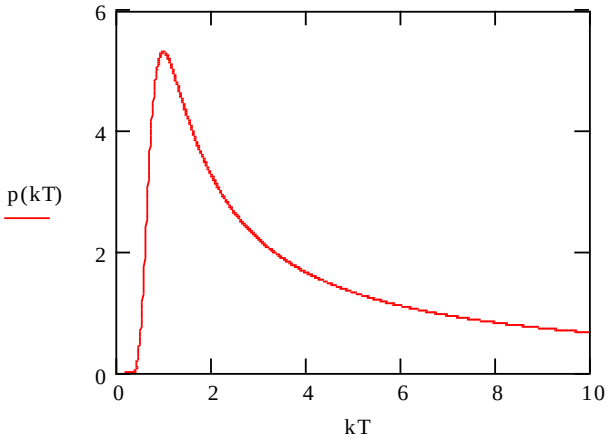

Fig. 1. The amplitude of the concentration (probability) vs. noise strength

This means that there is definite noise strength where the amplitude is maximal.

When we modulate a large frequency signal (carrier frequency) with a low frequency, we use the Taylor expansion up to the second order for equation (20), generating:

$$2\tau\frac{dp_1}{dt}=-(2+\left(\frac{\Delta E}{kT}\right)^2)p_1+1-\frac{\Delta E}{kT}+\frac{1}{2}\left(\frac{\Delta E}{kT}\right)^2, \tag{26}$$

$$2\tau=\left(Ce^{-\frac{E_0}{kT}}\right)^{-1}$$

The modulated electric field-strength is used as a harmonic function over time and the energy has to depend on it linearly, so:

$$\Delta E=a(1+m\cos\Omega t)\sin\omega t \tag{27}$$

where $m<1$ is the depth of the modulation, and Ω and ω are the circular frequencies of the modulation signal and the carrier wave, respectively.

$$2\tau\frac{dp_1}{dt}=-(2+\left(\frac{a}{kT}\right)^2(1+m\cos\Omega t)^2\sin^2\omega t)p_1+ \tag{28}$$

$$+1-\frac{a}{kT}(1+m\cos\Omega t)\sin\omega t+\frac{1}{2}\left(\frac{a}{kT}\right)^2(1+m\cos\Omega t)^2\sin^2\omega t,$$

$$2\tau=\left(Ce^{-\frac{E_0}{kT}}\right)^{-1}$$

Now, the time function of the concentration has two independent fluctuations: a slow one from the modulation and a quick one as a consequence of the carrier wave.

By averaging the high-frequency carrier signal, the slow signal can be considered as constant, so we obtain:

$$2\tau\frac{dp_1}{dt}=-(2+\left(\frac{a}{\sqrt{2}kT}\right)^2(1+m\cos\Omega t)^2)p_1+ \tag{29}$$

$$+1+\frac{1}{2}\left(\frac{a}{\sqrt{2}kT}\right)^2(1+m\cos\Omega t)^2$$

$$2\tau=\left(Ce^{-\frac{E_0}{kT}}\right)^{-1}$$

ISSN 2347-6893
Volume 9 Number2
Journal of Advances in Biology

When the modulation depth is small, a further simplification can be introduced, obtaining a linear differential equation with varying coefficients:

$$2\tau\frac{dp_1}{dt} = -(2+\left(\frac{a}{\sqrt{2}kT}\right)^2(1+2m\cos\Omega t))p_1 + \tag{30}$$
$$+1+\frac{1}{2}\left(\frac{a}{\sqrt{2}kT}\right)^2(1+2m\cos\Omega t)$$

We are looking for resonances, so we limit our attention to the harmonic excitation function, using successive approximation.

$$2\tau\frac{dp}{dt}+[2+\left(\frac{a}{\sqrt{2}kT}\right)^2+\left(\frac{a}{kT}\right)^2 m\cos\Omega t]p = \tag{31}$$
$$=\left(\frac{a}{\sqrt{2}kT}\right)^2 m\cos\Omega t$$

Introducing the expressions:

$$F(p) := 2\tau\frac{dp}{dt}+[2+\left(\frac{a}{\sqrt{2}kT}\right)^2+]p, \tag{32}$$
$$f(p) := p\left(\frac{a}{kT}\right)^2 m\cos\Omega t$$

Which are continuous additive functions of p.

Steps of successive approximation are:

$$F(p_1) = \left(\frac{a}{\sqrt{2}kT}\right)^2 m\cos\Omega t, \tag{33}$$
$$F(p_2) = f(p_1),$$
$$F(p_i) = f(p_{i-1})$$

Where we have:

$$F(p_1)+F(p_2)+..+F(p_i) = F(p_1+p_2+...+p_i) = \tag{34}$$
$$\left(\frac{a}{\sqrt{2}kT}\right)^2 m\cos\Omega t + f(p_1)+f(p_2)+...+f(p_{i-1}) =$$
$$=\left(\frac{a}{\sqrt{2}kT}\right)^2 m\cos\Omega t + f(p_1+p_2+...+p_{i-1})$$

ISSN 2347-6893
Volume 9 Number2
Journal of Advances in Biology

When the process is convergent than in case of i→∞ the expansion seeks to the solution and due to the requested continuity, equation (32) will be transformed to:

$$F(p)=\left(\frac{a}{\sqrt{2}kT}\right)^2 m\cos\Omega t + f(p) \tag{35}$$

The solution will be in the first approximation:

$$2\tau\frac{dp_1}{dt}+[2+\left(\frac{a}{\sqrt{2}kT}\right)^2+]p_1=\left(\frac{a\sqrt{m}}{\sqrt{2}kT}\right)^2\cos\Omega t \tag{36}$$

The amplitude of the probability changing by the modulating harmonic function will be:

$$\hat{p_1}(RT)=\left(\frac{a\sqrt{m}}{\sqrt{2}kT}\right)^2\frac{1}{\sqrt{4\tau^2\Omega^2+\left[2+\left(\frac{a}{\sqrt{2}kT}\right)^2\right]^2}}= \tag{37}$$

$$=\left(\frac{a\sqrt{m}}{\sqrt{2}kT}\right)^2\frac{1}{\sqrt{\left[2+\left(\frac{a}{\sqrt{2}kT}\right)^2\right]^2+\left(\frac{e^{\frac{E_0}{RT}}}{C}\Omega\right)^2}}$$

Which is again a well-formed resonance depending on the field strength of the modulating noise (Figure 2.).

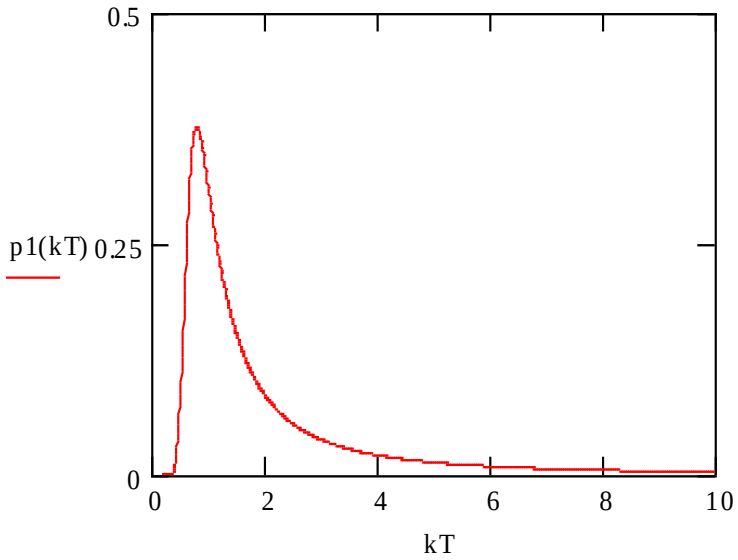

Fig. 2. The probability amplitude vs. noise strength in the first approximation

DISCUSSION

The above calculation had given rigorous proof that the amplitude-modulated carrier frequency is able to produce stochastic resonance, which could induce selectively various biological effects. For example, enzymatic reactions can be selectively excited, voltage-gated ion-channels can be activated or deactivated, and polymerization processes (like in the cytoskeleton) can be modified. Due to the huge number of various processes (enzymes, channels, etc.) and complex interconnections in bio-systems, the modification of complex processes is possible with an amplitude-modulated carrier.

Of course, the modulating signal could also be active alone, but its combination with high frequency could allow for selection deeper in the body. A low frequency alone does not penetrate well due to the impedance barrier of the skin, by which the carrier frequency could be overbridged. Also, various other selections, which are connected to higher frequencies (e.g. beta and delta dispersions [13]) could select for various tissues [14] and with these targets even various clusters [15] or cells [16]:, allowing for selective action on their cell membranes [17] by the construction of a well-controlled nano-effect by an electromagnetic field [18], [19].

REFERENCES

[1] Okamura, Y., Murata, Y., Iwasaki H. 2008. Voltage-sensing phosphatase: Actions and potentials. The Journal of Physiology. 587 (3): 513–520.

[2] Okamura Y. 2009. Voltage-sensing phosphatase: actions and potentials. J. Physiol. 587.3, 513–520.

[3] Drewes, G. et al. 1998. MAPs, MARKs and microtubule dynamics. Trends in Biochemical Sciences. 23:307–311.

[4] Levin, M. 2007. Large-scale biophysics: ion flows and regeneration. Trends Cell Biol. 17:261-270; Epub 2007.

[5] Bingelli, R., Cameron, IL. 1980. Cellular potentials of normal and cancerous fibroblasts and hepatocytes. Cancer Research. 40, 1830-1835.

[6] Chernet, BT., Levin, M. 2013. Transmembrane voltage potential is an essential cellular parameter for the detection and control of tumor development in a Xenopus model. Disease Models & Mechanisms. 6, 595-607.

[7] Simpson, RJ., Adams, PD., Golemis, EA. 2009. Basic Methods in Protein Purification and Analysis. CSH Press.

[8] Titushkin, I., Cho, M. 2009. Regulation of Cell Cytoskeleton and Membrane Mechanics by Electric Field: Role of Linker Proteins. Biophysical Journal. 96:717–728.

[9] Mycielska, ME., Djamgoz, MBA. 2004. Cellular mechanisms of direct-current electric field effects: galvanotaxis and metastatic disease. Journal of Cell Science. 117:1631-1639.

[10] Cho, H., Tharfe, HS., Lee, RC., Goland, DE. 1996. Reorganization of microfilament structure induced by ac electric fields. FASEB J. 10:1552-1558.

[11] Szasz, A., Szasz, N., Szasz, O. 2010. Oncothermia – Principles and Practices. Springer, Heidelberg.

[12] Adey, WR. 1984. Nonlinear, nonequilibrium aspects of electromagnetic field interactions at cell membranes. In: Adey, WR., Lawrence, AF. (eds) Nonlinear Electrodynamics in Biological Systems. Plenum Press, New York, London, 3-22.

[13] Schwan, HP. 1963. Determination of biological impedances. In: Physical Techniques in Biological Research. Vol. 6, Academic Press, New York, 323-406.

[14] Scott, GC., Joy, MG., Armstrong, RL., Henkelman, RM. 1995. Electromagnetic considerations for RF current density imaging [MRI technique]. IEEE Trans Med Imaging. 14:515-524.

[15] Vander Heiden, MG., Cantley, LC., Thompson, CB. 2009. Understanding the Warburg effect: The metabolic requirements of cell proliferation. Science. 324(5930):1029-1033.

[16] Szentgyorgyi, A. 1978. The living state and cancer. Marcel Dekker Inc, New York.

[17] Szasz, O., Szasz, A. 2014. Oncothermia - Nano-heating paradigm. J. Cancer Sci. Ther. 6:4.

[18] Szasz, A. 2013. Electromagnetic effects in nanoscale range. Cellular Response to Physical Stress and Therapeutic Applications (eds. Shimizu, T. Kondo, T.), chapter 4. Nova Science Publishers, Inc.

[19] Szasz, A. 2015. Bioelectromagnetic Paradigm of Cancer Treatment Oncothermia. In: Rosch, PJ. (ed) Bioelectromagnetic and subtle energy medicine. pp. 323-336, CRC Press, Taylor & Francis Group.

ISSN 2347-6893
Volume 9 Number2
Journal of Advances in Biology

Author' biography with Photo

Andras SZASZ

Prof. Dr. András Szász is the developer of the method oncothermia. He is educator; presently teaches at 3 different universities (St. Istvan University, Hungary; Pazmany P. University, Hungary; and Chiba University, Japan). He is head of the Department of Biotechnics in St. Istvan University. His research activity covers bioelectomagnetics and fractal physiology. The number of his publications is over 400 including books and articles.

DOI : 10.24297/jab.v9i2.4059